On as-built microstructure and necessity of solution treatment in additively manufactured Inconel 939

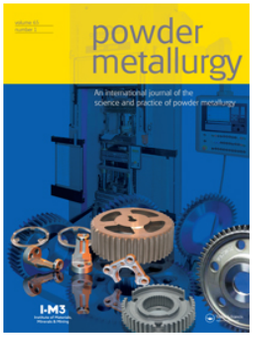

Powder Metallurgy

ISSN: (Print) (Online) Journal homepage: https://www.tandfonline.com/loi/ypom20

On as-built microstructure and necessity of solution treatment in additively manufactured Inconel 939

Abdul Shaafi Shaikh, Masoud Rashidi, Kevin Minet-Lallemand & Eduard Hryha

To cite this article: Abdul Shaafi Shaikh, Masoud Rashidi, Kevin Minet-Lallemand & Eduard Hryha (2022): On as-built microstructure and necessity of solution treatment in additively manufactured Inconel 939, Powder Metallurgy, DOI: 10.1080/00325899.2022.2041787

To link to this article: https://doi.org/10.1080/00325899.2022.2041787

Published online: 21 Feb 2022.

POWDER METALLURGY
https://doi.org/10.1080/00325899.2022.2041787

I·M3 Institute of Materials, Minerals & Mining
Taylor & Francis Taylor & Francis Group

On as-built microstructure and necessity of solution treatment in additively manufactured Inconel 939

Abdul Shaafi Shaikh [a,b], Masoud Rashidi [a], Kevin Minet-Lallemand [b] and Eduard Hryha [a]

[a]Department of Industrial and Materials Science, Chalmers University of Technology, Gothenburg, Sweden; [b]Electro Optical Systems Finland Oy, Turku, Finland

ABSTRACT

Increased adoption of additively manufactured superalloys has led to the consideration of revised heat treatment approaches for these materials. The rapid cooling during additive manufacturing processes has been seen to suppress gamma prime (γ') precipitation, which has raised the possibilities for omitting the high-temperature solution treatment step that usually precedes ageing heat treatment for these alloys. In this work, the as-built microstructure of a high gamma prime fraction superalloy Inconel 939 is presented, where the absence of any γ' precipitation is notable. However, transmission electron microscopy shows the presence of nano-sized Eta (η) phase. It is shown that the omission of solution treatment leads to the growth of the deleterious η phase upon ageing, which results in embrittlement in tensile loading. It is concluded that at least for this particular alloy the solution treatment plays a critical role in the establishment of the required microstructure and hence cannot be omitted from the heat treatment.

ARTICLE HISTORY
Received 26 November 2021
Accepted 9 February 2022

KEYWORDS
Additive manufacturing; laser powder bed fusion; superalloy; Inconel 939; heat treatment; TEM; microstructure development

Introduction

Recent progress in additive manufacturing (AM), or 3D printing, has led to a shift in the design and manufacturing of high-end components. AM enables the manufacture of complex shapes directly from a CAD model, without the need for preparation of tooling or moulds. Thus, AM enables faster prototyping and design-to-production cycles. AM technologies also allow greater design freedom than can be achieved with conventional manufacturing processes, as they are layer-wise processes. The most widely adopted and industrialised AM technology for metal materials is Laser Powder Bed Fusion (LPBF). The LPBF process involves metal powder which is spread over a substrate and then melted in the profile of the desired component by a high-powered laser. Further layers are added repeatedly and fused into underlying layers until the desired final shape is produced. LPBF can produce material which is virtually defect-free, with density and mechanical properties comparable to or exceeding those produced by conventional manufacturing processes.

One of the earliest adopted classes of materials in LPBF has been Ni-base superalloys for use in aeroengines and land-based gas turbines. Ni-base superalloys are a unique class of materials which maintain a combination of corrosion/oxidation resistance and strength at high temperatures. The high-temperature strength and resistance to creep and fatigue are typically achieved by precipitation strengthening of the γ matrix by the γ' intermetallic phase. Superalloys having high volume fractions of the γ' phase are typically manufactured by casting. After casting the as-solidified microstructure typically contains γ' phase and γ–γ' eutectic, due to the slow cooling during the casting process. The castings are then given a solution treatment to form a super-saturated solid solution, which is subsequently aged to precipitate the strengthening phase.

The study of the microstructure of γ'-strengthened superalloys directly after manufacture by LPBF (i.e. in the 'as-built' condition) has shown the absence of γ' precipitates [1–4]. This is understood to be because of the fast cooling rates during the LPBF process, which results in suppression of the diffusion-driven precipitation reaction [5]. These findings have led researchers to suggest that full solution heat treatments may not be necessary for LPBF processed Ni-base superalloys, and alternative sub-solvus heat treatments have been proposed for some alloys [1,6,7].

Skipping the solution treatment step or reducing the temperature of heat treatment can be desirable for large-scale manufacturing of Ni-base superalloy components since the heat treatment step can be time consuming, energy intensive, and thus expensive. High-temperature heat treatments also pose the risk of

CONTACT Abdul Shaafi Shaikh abdulsh@chalmers.se Electro Optical Systems Finland Oy, Lemminkäisenkatu 36, 20520 Turku, Finland

Table 1. Nominal chemical composition of IN939.

IN939	Ni	Cr	Co	Ti	Al	Nb	Ta	W	Zr	B	C
wt-%	Bal	22.5	19	3.7	1.9	1.0	1.4	2.0	0.1	0.01	0.15

incipient melting in Ni-base superalloys. Therefore, there exist economic and technical incentives to promote omitting full solution treatments from the heat treatment regimes of LPBF Ni-base superalloys.

One of the first γ'-strengthened Ni-base superalloys to be adopted for LPBF is Inconel 939 (IN939) [8]. IN939 was developed as an investment casting superalloy for use in gas turbine hot sections at temperatures up to 850°C, with emphasis on corrosion and oxidation resistance, while retaining excellent mechanical properties owing to precipitation strengthening by the γ' phase. Solution treatment of IN939 is done at temperatures of 1160°C or above and is usually the first of multiple steps. Therefore, skipping this step would be especially beneficial in the case of IN939 produced by LPBF. However, it is important to note that in the case of cast IN939, the solution treatment is performed not only for dissolution of γ' formed during solidification (dissolving at around 1100°C), but also to remove the deleterious Eta (η) phase from the microstructure.

The η phase in IN939 and other superalloys has been studied and reported extensively in the literature. This phase is typically observed in platelet morphology, has a hexagonal DO24 crystal structure and is usually given the form Ni_3Ti [9]. Bouse et al. described the formation of η phase in cast IN939 vanes, suggesting the phase as being responsible for low room temperature tensile ductility as well as low creep ductility [10]. Formenti et al. through thermal analysis demonstrated that η forms as a eutectic solidification product in IN939. The chemical composition of η was shown to be high in Ni and Ti, while also containing some Cr and Co [11]. Jahangiri et al. showed the morphology of η at interdendritic regions in the microstructure and exposed the deleterious effects of incipient melting caused by the high solution treatment temperature [12,13]. Additional work by Jahangiri et al. also found that the 'standard' 1160°C solution treatment was not sufficient to dissolve η, and an alternative and lengthy solution heat treatment to remove the phase was proposed [14]. Kanagarajah et al. studied the microstructure of LPBF IN939 and showed a platelet-like phase in the microstructure, described as a 'brittle phase', expected to be η-phase [15]. Apart from the embrittling effects of η, it is known that the formation of η is more likely in alloys with higher levels of Ta and Ti. A lower carbon content, as well as a lower ratio of Ti to Al content, can decrease the propensity of η formation [10,16].

To understand the feasibility of omitting a solution treatment for IN939, a clear picture of the starting microstructure is required. In particular, it needs to be understood what phases are present, and especially whether γ' and η phases form upon solidification, and it is these questions which are addressed in this communication.

It is pertinent to note that η phase can also be formed in the microstructure of superalloys by reactions of γ' after extended periods of high-temperature exposure, and this transformed occurrence of η phase is not the subject of discussion in this article as such exposure is not possible either during LPBF nor during heat treatment.

Materials and methods

Samples for microstructural analysis and mechanical testing were built in an EOS M290 (Electro Optical Systems GmbH, Krailling, Germany) LPBF system using the IN939_040_HiPerM291_1.00 parameter set. Pre-alloyed gas atomised IN939 powder supplied by EOS and having d_{50} of 32 μm was used. The nominal chemical composition of IN939 is given in Table 1. Samples were built in the form of cubes of dimension $15 \times 15 \times 15$ mm^3, and cylinders of 11 mm diameter and 80 mm length with orientation perpendicular to the building direction.

Heat treatments were performed in a Nabertherm N41/H model box furnace under Ar gas atmosphere. Solution treatment was performed at 1190°C for 4 h, followed by rapid cooling with pressurised air. Two-step ageing treatment involved soaking at 1000°C for 6 h, followed by air cooling and soaking at 700°C for 16 h, also followed by air cooling. Heat treatment steps are schematically illustrated in Figure 1. As-built samples were subjected to two different heat treatment regimes: (1) direct ageing, or (2) solution treatment + ageing.

An FEI Titan 80-300 TEM equipped with an EDAX X-ray detector and TIA EDS software was employed for detailed characterisation of the manufactured specimens in the as-built condition. The FEI Titan TEM was operated at 300 kV. To prepare electron transparent specimens for TEM investigations, discs of 3 mm in diameter were cut and mechanically ground and polished to a thickness of 0.1 mm. Discs were further electrochemically polished in a 10% perchloric acid + 90% methanol using twin-jet Struers Tenupol 5.

Samples for optical microscopy and scanning electron microscopy (SEM) analysis were cross-sectioned in planes parallel or perpendicular to the building direction, and metallographic preparation was done by mounting in conductive epoxy and grinding and

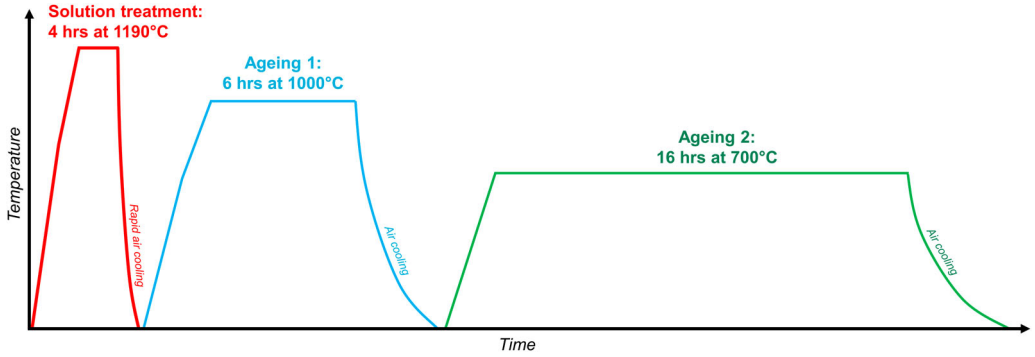

Figure 1. Schematic illustration of heat treatment steps used for LPBF produced IN939 in this study.

polishing to 1 µm finish. Etching was performed with Kalling's 2 reagent. Optical microscopy was performed with an Olympus GX51 microscope, and SEM analysis with a Zeiss Gemini-SEM450. Energy Dispersive X-ray Spectroscopy (EDX) analysis was performed with a Bruker FlatQuad detector mounted in the said microscope.

Tensile testing at room temperature was performed according to ISO 6892-1, in crosshead control mode with a strain rate of 0.00025/s up to yield and 0.002/s to fracture. Tensile samples were machined to the dimensions according to ASTM E8M Standard Round Machined Tension Test Specimen for P/M Products, with gauge length 25.4 mm and gauge diameter 4.75 mm. Three samples were tested for each heat treatment condition.

Results

The IN939 material manufactured by LPBF showed columnar grains elongated along the building direction, and a fine dendritic microstructure, as seen in Figure 2. Dendrites growing along the build direction were clearly visible in sections parallel to the building direction, see Figure 2(b), and arrays of sub-micron sized particles at the interdendritic regions could be seen. In sections perpendicular to the building direction, see Figure 2(c), the dendrite core and interdendritic region can be distinguished, and several small particles with various morphologies are visible at the interdendritic region.

TEM analysis showed that the as-built material has a high density of dislocations, especially at interdendritic regions. A grain boundary region is shown in Figure 3(a). The difference in growth orientations of dendrites on either side of the boundary is clearly visible. Particles arrayed along the interdendritic regions and grain boundary can be seen in darker contrast. The apparent absence of dislocations in the grain on the right side of the micrograph is probably due to the preferential orientation of the sample to the electron beam.

No precipitates of the γ' phase could be seen in the microstructure with SEM or TEM. Electron diffraction patterns from the dendrite core, see Figure 3(b), did not show any superlattice reflections, indicating only γ phase.

High resolution imaging of the interdendritic regions showed that these regions typically contained several particles within a very small volume. Figure 3(c) shows an example of an interdendritic location with multiple nano-sized particles. Two distinct morphologies can be observed at interdendritic regions overall: a 'blocky' morphology of roughly equiaxed particles and an elongated or 'platelet' morphology. Additional examples of particles with such distinct morphologies can be seen in Figure 3(d,e), further exemplifying the difference in proportions and aspect ratio between the particles of the respective morphologies.

Examination of the two different particle morphologies was performed by TEM-EDX analysis, results of which are shown in Figure 4. The particles with blocky morphology were found to exhibit a marked enrichment of C, Ti, Ta and Nb, as seen from the prominent peaks in the EDX spectrum. This composition suggests that these particles are MC carbides. EDX spectra from the elongated particles showed strong peaks of Ti and Ni, along with matrix elements Cr and Co. The strong indication of matrix elements suggests that due to the small thickness of the particle, the interaction volume of the electron beam generating the spectrum included the matrix. However, the strong Ti and Ni peaks relative to the Ta and Nb peaks suggest a Ni- and Ti-based intermetallic phase. Based on this composition, morphology, and the characteristics of η phase determined by other researchers [17,18], this phase is likely be η phase. To investigate the effects of thermal exposure on this phase, and to further confirm its composition, ageing of the as-built microstructure was performed and effect on the suspected η phase was observed.

Bulk precipitation of a plate-like phase was observed in the microstructure of the material aged (1000°C/6 h + 700°C/16 h) without solution treatment. Individual platelets could be observed in SEM

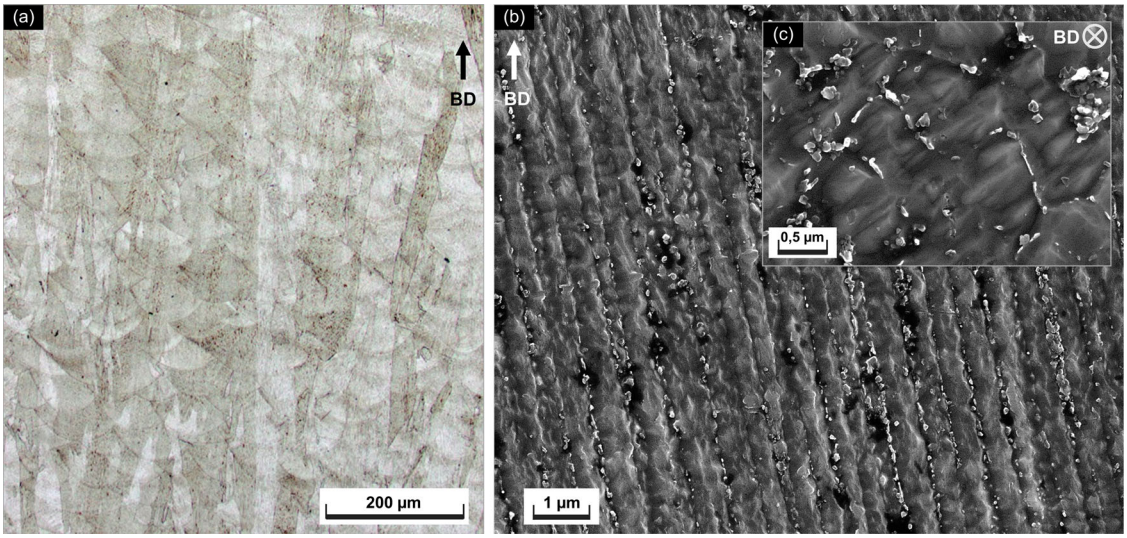

Figure 2. Microstructure of IN939 in the as-built condition, (a) optical micrograph, (b,c) SEM micrographs with secondary electron detector. Kalling's 2 etch. Arrow indicates building direction.

imaging, as shown in Figure 5, along with several other phases which are commonly observed in the heat treated microstructure of IN939. EDX analysis in SEM showed that the platelets are enriched in Ti and Ni. Weak indications of Ta and Nb were also detected. Spherical precipitates of 200–300 nm in diameter were seen to be rich in Ni, Ti and Al, and were thus identified as γ' phase. Carbides were identified by their bright contrast relative to the matrix and by their enrichment in Ti, Ta and Nb.

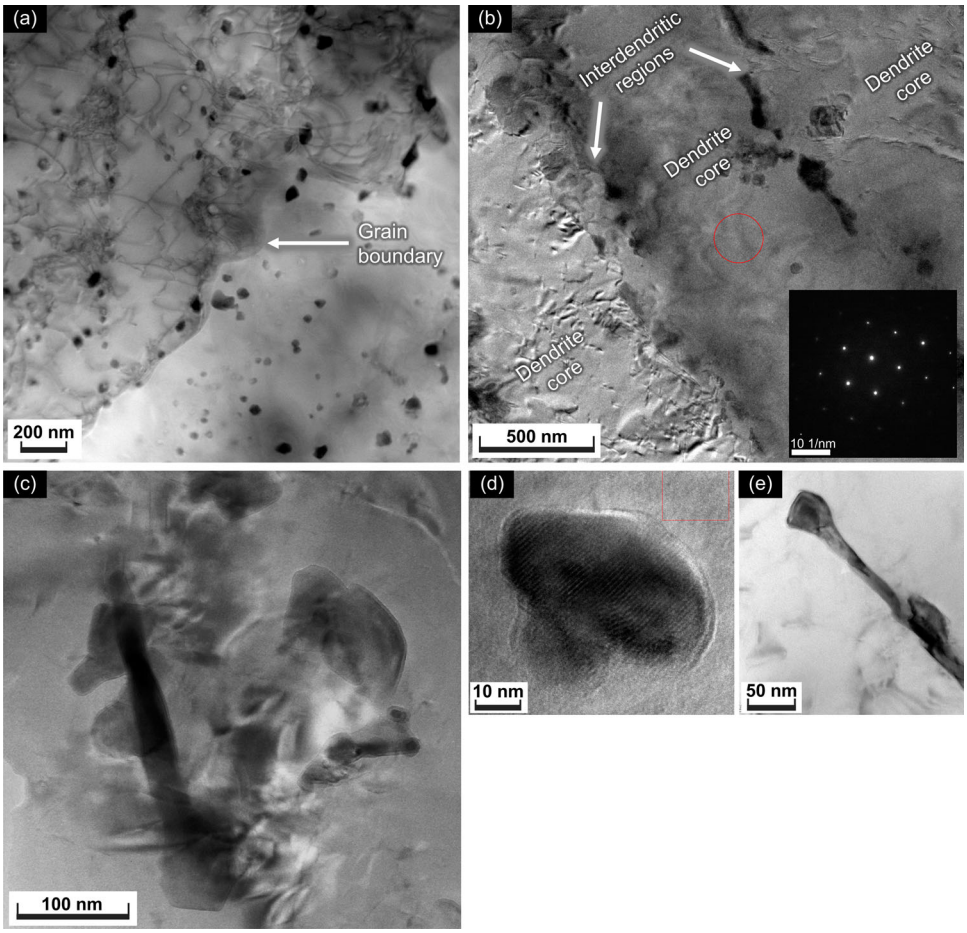

Figure 3. (a) TEM bright-field (BF) micrograph of a grain boundary region in as-built IN939; (b) dendritic microstructure in BF imaging, inset shows diffraction pattern, showing absence of superlattice reflections; (c) a higher magnification micrograph of an interdendritic region, showing several particles with varying morphologies; (d) a particle with blocky morphology; (e) a particle with elongated/platelet morphology.

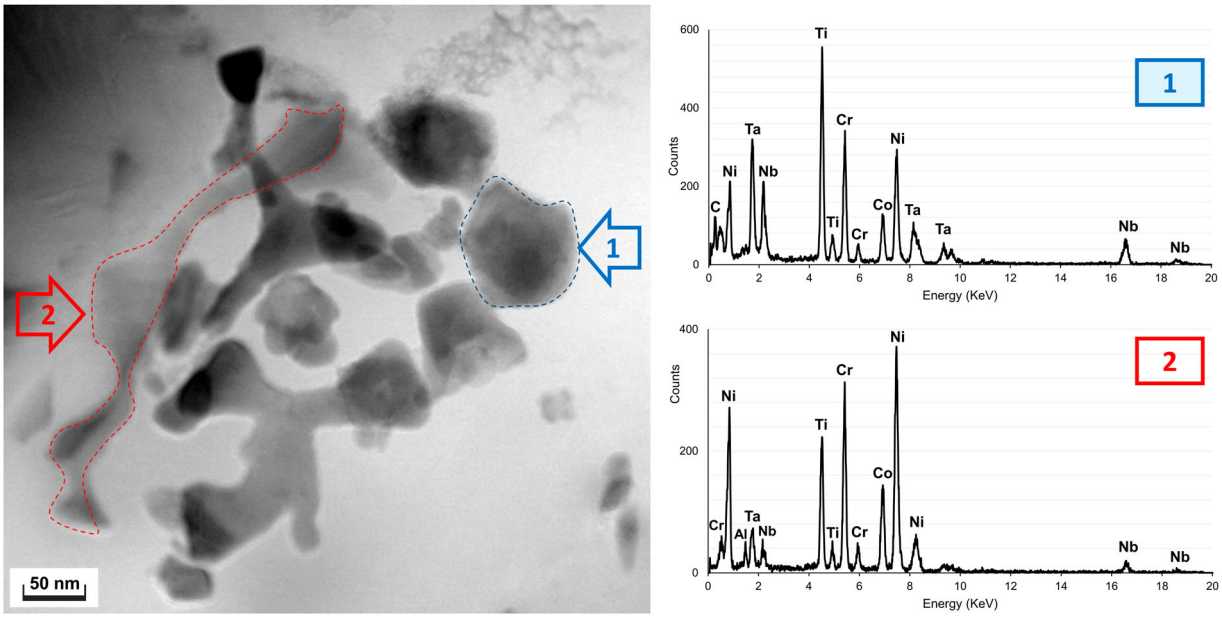

Figure 4. (a) TEM – BF micrograph showing an interdendritic region with several particles. EDX spectrum from blocky particle marked '1'; and EDX spectrum from elongated particle marked '2'.

On the other hand, no plate-like phase could be observed in the microstructure of material subjected to solution treatment + ageing (1190°C/4 h + 1000°C/6 hrs + 700°C/16 h). The SEM micrograph and corresponding EDX maps are displayed in Figure 6. The microstructure in this condition appears to contain γ/γ' within grains along with fine dispersed intragranular MC carbides rich in Ti, Ta and Nb. Larger carbides

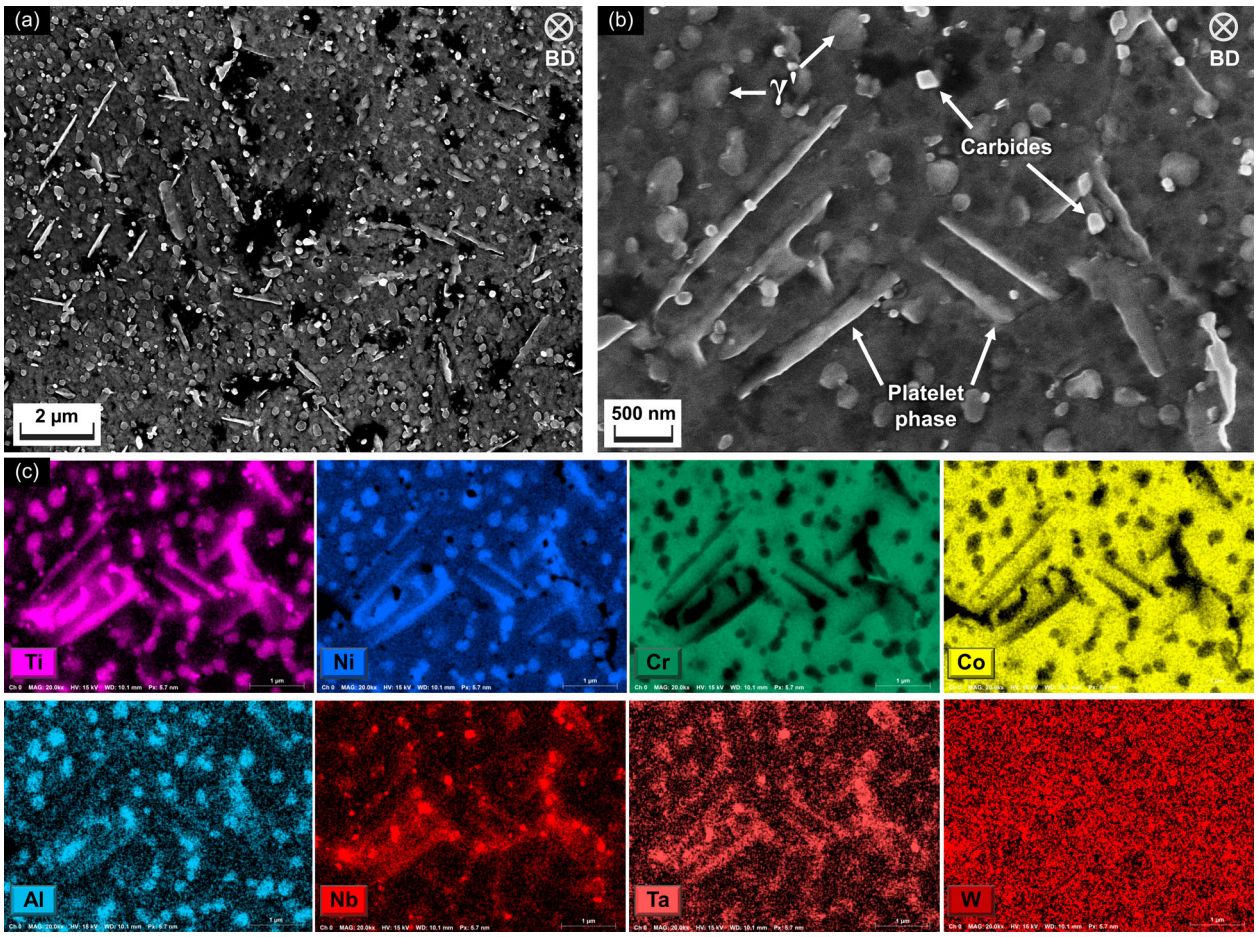

Figure 5. SEM micrographs showing microstructure of IN939 aged without solution treatment; (a,b) show microstructure from secondary electron detector; (c) EDX maps of microstructure from (b).

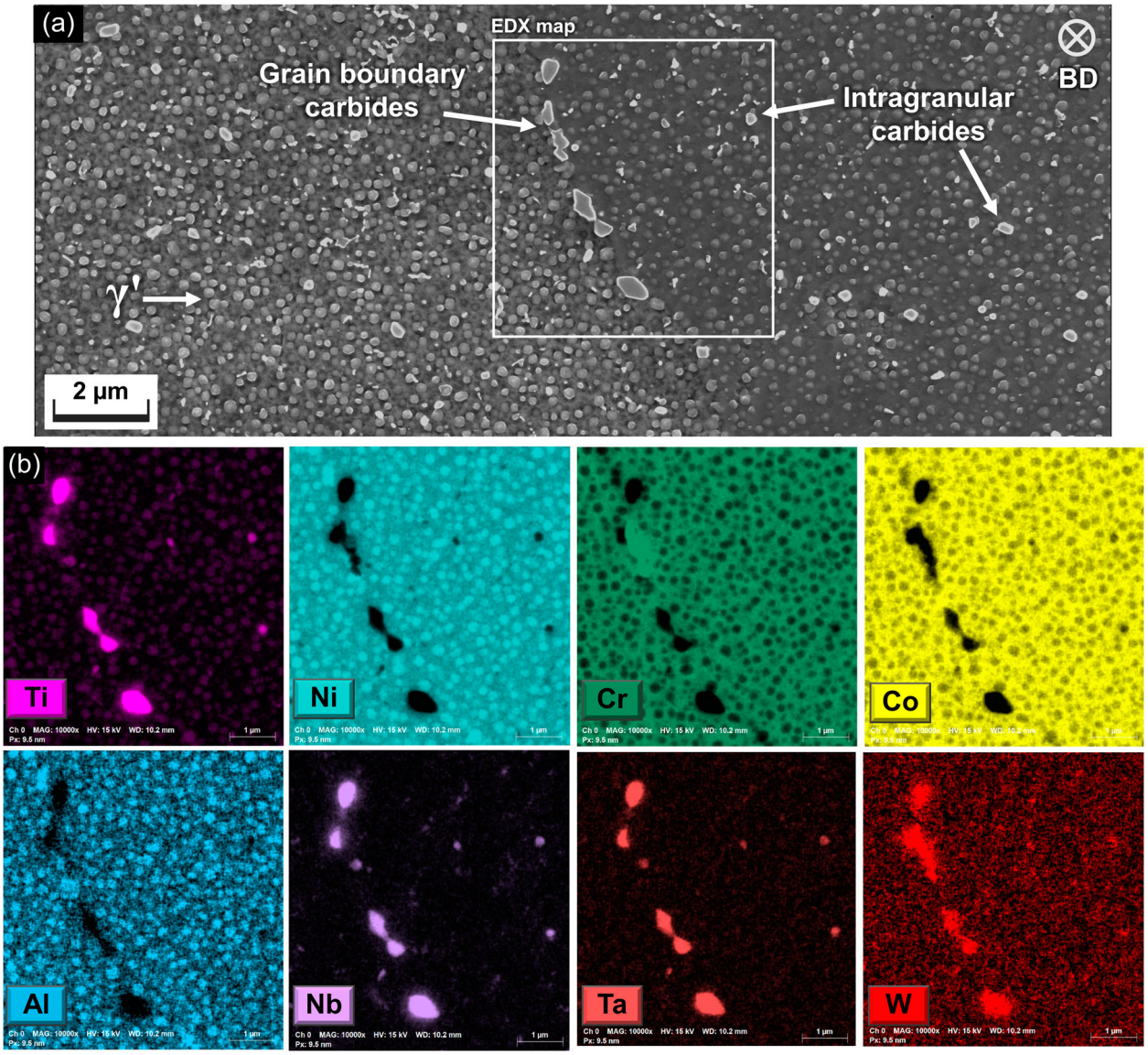

Figure 6. SEM micrographs showing microstructure of IN939 after solution treatment + ageing; (a) shows microstructure from secondary electron detector; (b) EDX maps of indicated region microstructure from (a).

were also observed at the grain boundaries, which were either MC (Ti, Ta and Nb rich), or $M_{23}C_6$ (Cr, W-rich). Note that the accuracy of W detection in EDX is known to be limited due to overlapping peaks of W and Ta, and the small alloying quantity of this element in IN939.

Tensile testing at room temperature was performed to understand the effect of the microstructure and observed precipitation of platelet phases on the mechanical performance of the alloy. Representative tensile curves of the material aged with and without solution treatment are shown in Figure 7, and mean values of yield strength, ultimate tensile strength, and elongation at fracture are given in Table 2. The material without solution treatment and containing platelet phases in addition to γ/γ' phases, exhibited lower elongation than material that had undergone solutionising before heat treatment. Subsequent fractography of the specimens after tensile testing showed trans-granular ductile failure with characteristic fine shallow dimples and the presence of large elongated dimples initiated by the platelet precipitates. These are observed as cracked platelets on the fracture surface, as depicted in Figure 7(c), while no platelet phase was observed on the fracture surfaces on specimens aged after solution treatment.

Discussion

The absence of any observable γ' precipitation in the as-built microstructure, even with high-resolution TEM, suggests that in IN939 the γ' precipitation reaction is indeed suppressed during the LPBF process. Note that samples for analysis were taken from mid-sections of the printed shapes, which would have undergone numerous thermal cycles due to the melting of subsequent layers. This result further corroborates reports by other works on AM of Ni-base superalloys with similar volume fractions of γ' [1–3]. Along with the absence of any γ–γ' eutectic, this result

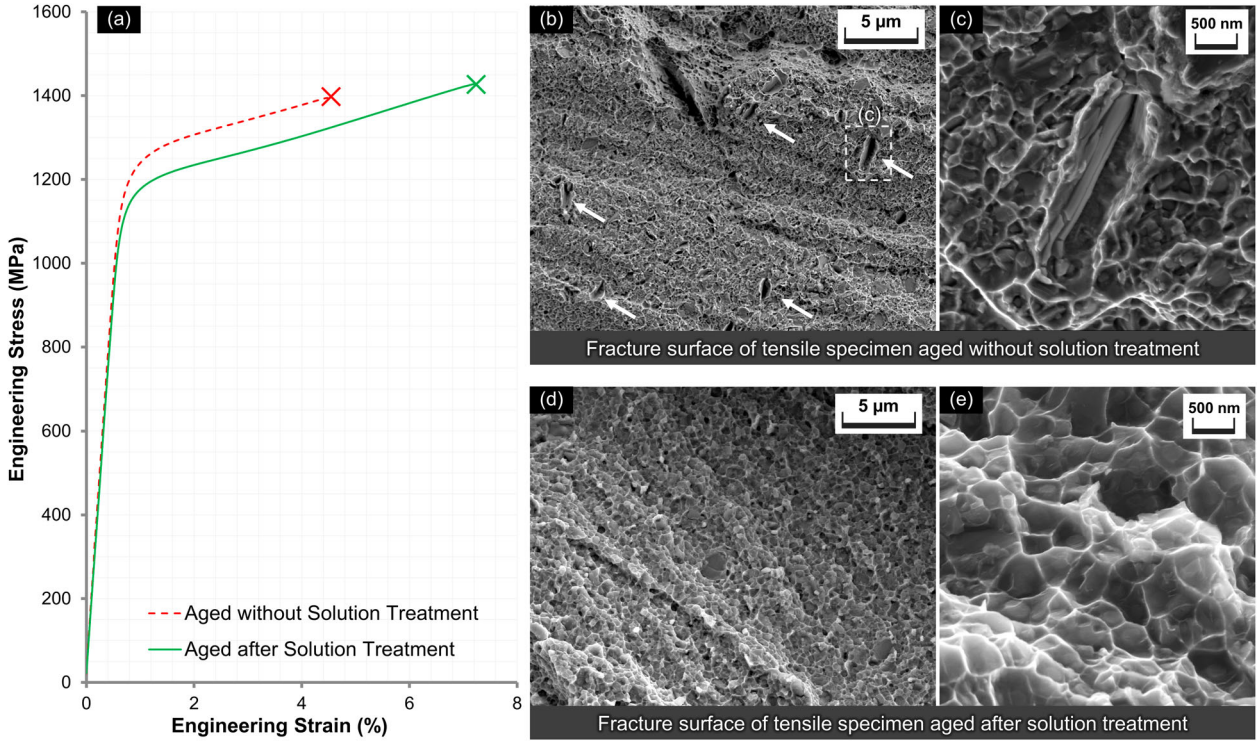

Figure 7. (a) Room temperature tensile testing curves from IN939 samples aged with and without solution treatment; (b,c) fracture surface of tensile specimen aged without solution treatment; (d,e) fracture surface of tensile specimen aged after solution treatment.

supports the idea that a full solution treatment may be unnecessary for this alloy.

A phase with platelet morphology was observed at interdendritic regions in the as-built microstructure of IN939. This observation has not been reported in previous works. Through EDX analysis, it was determined that this phase is most likely to be the Ni_3Ti – η phase. To confirm this hypothesis, the material was aged without solution treatment and characteristic platelets were observed at interdendritic regions, which were further confirmed to be Ni and Ti rich. This provides further confirmation that the observed platelets are η phase. Previous accounts of η phase in cast IN939 show the phase in the as-solidified microstructure to be up to several tens of microns in length, corresponding to the course as-cast microstructure [11,14]. However, the η phase platelets observed in the as-built LPBF IN939 in the current work were sub-micron sized, but more widely spread, corresponding to the fine microstructure resulting from fast cooling rates during the LPBF process. In the aged LPBF microstructure, precipitation of η phase can be explained by the larger number of interdendritic sites per volume of material, where η phase platelets are formed upon solidification, and where they grow in size during ageing. The particular morphology observed has been referred to in the literature as 'Widmanstätten' or 'intra-granular platelet' morphology [16].

Another feature of the as-built microstructure was MC carbides with a characteristic blocky morphology, observed at interdendritic regions, which has been reported also by other authors [19,20]. The carbides were also identified through their composition, and similar to η were observed to increase in size after ageing heat treatment. A high dislocation density was also observed, and this has also been reported by other authors in similar alloys [21].

Despite the small size of the η particles observed, tensile testing clearly showed the embrittling effect of the η phase on the material. This effect is well reported in the literature [10,16,18] and it is expected that the severity would be increased at higher temperatures and with extended thermal exposure. While not directly observed in the current work, it can also be expected that binding of Ti in η phase will result in the reduction of γ' volume fraction and consequent degradation of high-temperature strength.

Based on the above discussion, it is suggested that while solution treatment in LPBF IN939 may not be necessary for the dissolution of the γ' phase, it has a

Table 2. Mean values (± standard deviation) of tensile testing results of IN939 after direct ageing and after solution treatment + ageing.

	$R_{p0.2}$ (MPa)	R_m (MPa)	A%
Direct aged	1214 ± 7	1429 ± 35	4.6 ± 0.90
Solution treated + aged	1149 ± 2	1438 ± 10	6.4 ± 0.02

Yield strength is $R_{p0.2}$, Ultimate tensile strength is R_m and elongation at fracture is A%.

vital role in removing the η phase from the microstructure, and as such cannot be omitted. The solution treatment is likely to provide other benefits as well, such as homogenisation of chemical composition across the dendrite cores and interdendritic regions, relief of residual stresses and possible recrystallisation of the fine-grained microstructure [22]. Alloys other than IN939 may still benefit from sub-γ'-solvus heat treatments directly after printing, as their compositions may be unlikely to form detrimental phases like η.

Conclusions

As-built microstructure of LPBF IN939 was examined by TEM to determine the suitability of the microstructure for ageing without solution treatment. No γ' precipitates could be found; however, sub-micron sized platelet precipitates were observed in the interdendritic regions. These were identified by compositional analysis to be η phase. The phase was observed to grow rapidly during ageing without solution treatment and was found to have a detrimental effect on ductility. Based on the results of this study, it can be concluded that while solution treatment may not be necessary for the dissolution of γ', it is still required in order to achieve a stable microstructure free of detrimental η phase.

Disclosure statement

No potential conflict of interest was reported by the author(s).

Funding

This work has been performed in the framework of the Centre for Additive Manufacturing – Metal (CAM^2), financed by Vinnova [grant number 2016-05175].

Notes on contributors

Abdul Shaafi Shaikh is a materials engineer and industrial doctoral student at EOS Metal Materials and Chalmers University of Technology. His research focuses on additive manufacturing (3D printing) of nickel-base superalloys for high-temperature applications. Shaafi's research is conducted as part of the CAM^2 competence centre for additive manufacturing.

Dr. *Masoud Rashidi* is a materials scientist with extensive experience in physical metallurgy and additive manufacturing of high-temperature materials, as well as expertise in electron microscopy and atom probe tomography.

Kevin Minet-Lallemand is a materials scientist and Technology Development Manager at EOS Metal Materials in Finland, focusing on developing new metal materials and processes for Laser Powder Bed Fusion Additive Manufacturing. He has more than a decade of experience in process development, powder analysis and statistical process control of additively manufactured Ni-base superalloys.

Professor *Eduard Hryha* is a researcher in powder metallurgy and metal additive manufacturing. His research focuses on powder metallurgy, powder-based metal additive manufacturing, surface analysis using advanced surface-sensitive techniques, as well as thermal analysis. He is also a director of CAM^2 competence centre focusing on powder-based metal additive manufacturing.

ORCID

Masoud Rashidi http://orcid.org/0000-0001-8683-349X
Kevin Minet-Lallemand http://orcid.org/0000-0002-5069-0535
Eduard Hryha http://orcid.org/0000-0002-4579-1710
Abdul Shaafi Shaikh http://orcid.org/0000-0001-6017-6698

References

[1] Tang YT, Panwisawas C, Ghoussoub JN, et al. Alloys-by-design: application to new superalloys for additive manufacturing. Acta Mater. 2021;202:417–436.
[2] Jägle EA, Sheng Z, Wu L, et al. Precipitation reactions in Age-hardenable alloys during laser additive manufacturing. JOM. 2016;68:943–949.
[3] Luca Ad, Kenel C, Griffiths S, et al. Microstructure and defects in a Ni-Cr-Al-Ti γ/γ' model superalloy processed by laser powder bed fusion. Mater Des. 2021: 109531.
[4] Tang YT, Ghoussoub JN, Panwisawas C, et al. The effect of heat treatment on tensile yielding response of the new superalloy ABD-900AM for additive manufacturing. In: Tin S, Hardy M, Clews J, editors. Superalloys 2020. Cham, Switzerland: Springer International Publishing AG; 2020. p. 1055–1065.
[5] Hocine S, van Swygenhoven H, van Petegem S, et al. Operando X-ray diffraction during laser 3D printing. Mater Today. 2020;34:30–40.
[6] Wessman A, Cormier J, Hamon F, et al. Microstructure and mechanical properties of additively manufactured Rene 65. In: Tin S, Hardy M, Clews J, editors. Superalloys 2020. Cham, Switzerland: Springer International Publishing AG; 2020. p. 961–971.
[7] Wang R, Zhu G, Tan Q, et al. Effect of high temperature aging on microstructures and tensile properties of a selective laser melted GTD222 superalloy. J Alloys Compd. 2021;853:157226.
[8] Bridges A, Shingledecker J, Torkaman A, et al. Metallurgical evaluation of an additively manufactured Ni-base superalloy for Gas tubrine guide vanes. Proceedings of ASME turbo expo 2020. 2020.
[9] Durand-Charre M. The microstructure of superalloys. Amsterdam: Gordon & Breach; 1997.
[10] Bouse GK. Eta (n) and platelet phases in investment cast superalloys. In: Kissinger RD, editor. Superalloys 1996. Seven Springs Mountain Resort, Pennsylvania, USA: Minerals, Metals & Materials Society; 1996. p. 163–172.
[11] Formenti A, Eliasson A, Mitchell A, et al. Solidification sequence and carbide precipitation in IN718, IN625, and IN939. Casting of Metals. 2005;24:239–258.
[12] Jahangiri MR, Boutorabi SMA, Arabi H. Study on incipient melting in cast Ni base IN939 superalloy during solution annealing and its effect on hot workability. Mater Sci Technol. 2012;28:1402–1413.

[13] Jahangiri MR, Arabi H, Boutorabi SMA. Development of wrought precipitation strengthened IN939 superalloy. Mater Sci Technol. 2012;28:1470–1478.
[14] Jahangiri MR, Arabi H, Boutorabi SMA. Investigation on the dissolution of η phase in a cast Ni-based superalloy. Int J Miner Metall Mater. 2013;20:42–48.
[15] Kanagarajah P, Brenne F, Niendorf T, et al. Inconel 939 processed by selective laser melting: effect of microstructure and temperature on the mechanical properties under static and cyclic loading. Mater Sci Eng A. 2013;588:188–195.
[16] Sims CT, Stoloff NS, Hagel WC. Superalloys II: high-temperature Materials for aerospace and Industrial power. New York: Wiley; 1987.
[17] Seo SM, Kim IS, Lee JH, et al. Eta phase and boride formation in directionally solidified Ni-base superalloy IN792 + Hf. Metall and Mat Trans A. 2007;38:883–893.
[18] Choi BG, Kim IS, Kim DH, et al. ETA phase formation during thermal exposure and Its effect on mechanical properties in Ni-base superalloy GTD 111. Superalloys 2004 (tenth international symposium) proceedings; 2004. p. 163–171.
[19] Marchese G, Parizia S, Saboori A, et al. The influence of the process parameters on the densification and microstructure Development of Laser Powder Bed fused Inconel 939. Metals (Basel). 2020;10:882.
[20] Shaikh AS. Development of a gamma prime precipitation hardening Ni-base superalloy for additive manufacturing [Masters Thesis]. Gothenburg, Sweden: Chalmers University of Technology; 2018.
[21] Xu J, Gruber H, Boyd R, et al. On the strengthening and embrittlement mechanisms of an additively manufactured nickel-base superalloy. Materialia. 2020;10:100657.
[22] Banoth S, Li C-W, Hiratsuka Y, et al. The effect of recrystallization on creep properties of alloy IN939 fabricated by selective laser melting process. Metals (Basel). 2020;10:1016.